

1 Paleocological insights on latest Oligocene-early Miocene planktonic foraminifera
2 from the J-Anomaly Ridge (IODP-Hole U1406A)

3 Alessio FABBRINI^{1*}, Luca Maria FORESI¹

4 ¹ Department of Physical Sciences, Earth and Environment, University of Siena, Via
5 Laterina 8, 53100 Siena, Italy

6 *Correspondence: fabbrini21@student.unisi.it

7 ORCIDs:

8 Alessio FABBRINI: <https://orcid.org/0000-0002-4190-6429>

9 Luca Maria FORESI: <https://orcid.org/0000-0002-3122-5363>

10
11 Abstract: This paper focuses on a paleoecological study conducted on planktonic
12 foraminifera from upper Oligocene-lower Miocene deposits of the J-Anomaly Ridge
13 (North Atlantic Ocean). Paleoclimatic studies are crucial to better comprehend how
14 climatic changes occurred in the past and how they might influence global climate in the
15 next few decades. Oceanic currents are the predominant vehicle for heat transport across
16 the globe, therefore organisms living within the water mass can supply a lot of
17 information on paleoceanographic settings. In total 53 samples from the IODP Hole
18 U1406A were selected in the core interval 96-24 CCSF-M to perform statistical analyses
19 (R-mode cluster analysis, Principal Component Analysis) to describe ecogroup
20 distribution and a paleoclimatic curve based on shallow dwelling taxa. The species have
21 been subdivided into three ecogroups referring to recent studies on planktonic
22 foraminiferal paleoecology. The statistical analyses allowed a preliminary screening of
23 the distribution of the foraminiferal assemblages in the biozonal interval O7-M3. The
24 ecogroup distribution curves revealed the behavior of each group along the section,
25 highlighting the interconnection among the various habitats. Finally, the abundance of

1 the surface taxa was used to trace a paleoclimatic curve (SDPC) describing the superficial
2 water variations. Those results were compared with the Alkenone-Sea Surface
3 Temperature (SST) record from IODP-Site U1404 and the $\delta^{18}\text{O}$ North Atlantic stack from
4 the literature. This comparison showed a good match among the foraminiferal and
5 geochemical data, allowing the correlation between SDPC and SST minima to well-
6 known glacial events of the North Atlantic Ocean. This study supports the potential of
7 census data of planktonic foraminifera in paleoclimatic studies, when geochemical data
8 are not available.

9 Key words: planktonic foraminifera, early Miocene, North Atlantic, Newfoundland
10 Ridge, paleoclimate, U1406

11 1. Introduction

12 The Newfoundland Ridge is a key study area to understand the Oligocene-Miocene
13 climatic history of the North Atlantic Ocean. In this area (Figure 1), the intersection of
14 the North Wall Gulf Stream, the Deep Western Boundary Current (Labrador Current) and
15 the Western Greenland Current plays a crucial role in the local and global climate,
16 influencing sedimentation and water circulation in the western portion of the Atlantic
17 Ocean and regulating thermohaline circulation (Boyle et al., 2017; Broecker, 1997;
18 Laskar et al., 1987; Townsend et al. 2004). Many authors have studied this area (Keller
19 et al., 1987; Miller et al., 1991; Wright et al., 1991, Boyle et al., 1987, 2017; Townsend
20 et al., 2004, among others) to describe the glacial events of the northern hemisphere
21 during the Neogene (cfr. Brunner and Maniscalco, 1998). The aim of this paper is to
22 contribute to understanding of the paleoecological evolution of this area during the early
23 Miocene, using planktonic foraminifera collected at IODP-Hole U1406A.

24 1.1 The J-Anomaly Ridge

1 Newfoundland Ridge (Canada) is a well-known study area due to its isolated position
2 from downslope sedimentation, typical of the Grand Banks and canyon areas, which
3 probably guarantees a more continuous stratigraphic record. The J-Anomaly Ridge
4 extends southwestward from the southeastern portion of the Newfoundland Ridge and
5 today is 4000 m deep. At this depth the oscillating Carbonate Compensation Depth (CCD)
6 has influenced sedimentation since the Paleogene, especially during the Miocene
7 (Maniscalco and Brunner, 1998), producing regional unconformities as described by
8 Miller et al. (1985) and Keller et al. (1987). The contouritic currents also created
9 significant regional hiatuses and unconformities during the Cenozoic (Boyle et al., 2017)
10 hindering biostratigraphic and paleoecological reconstructions. In this region the
11 sedimentary framework is determined by many factors. The sea floor is swept by the
12 North Atlantic Deep Water (NADW), a collective term indicating the cold and high
13 salinity water masses originated by sinking in the Labrador Sea and Greenland-
14 Norwegian Sea (Deep Western Boundary Current) as shown in Figure 1. These currents
15 cause contouritic sedimentation, displacing the sediments for kilometers (currents flow
16 >10 cm/s, Boyle et al., 2017). The interference of pelagic sedimentation with the oceanic
17 currents allowed the formation of thick sediment drifts (more than 2 Km) from the
18 Paleogene to the present (Boyle et al, 2017; Heezen and Hollister, 1964; Heezen et al.,
19 1966; Tucholke and Mountain, 1979; Mountain and Tucholke, 1985; Faugères et al.,
20 1999; Stow et al., 2002; Rebesco et al., 1991 and 2014). Despite their nature, the
21 contouritic deposits recorded all the major climatic events, such as the Eocene Thermal
22 Maximum (ETM), the Eocene-Oligocene climate transition, the Oligo-Miocene
23 Transition (OMT) and glacial-interglacial cycles during the Neogene. Understanding the
24 climatic evolution of this area may therefore provide a major contribution to the
25 paleoceanographic reconstruction of the North Atlantic Ocean.

1 In the Neogene, the late Oligocene-early Miocene represents a transitional interval.
2 Starting from the Eocene Thermal Maximum, global climate went through multiple
3 phases, until the latest Oligocene which was generally considered warm and ice free, but
4 glaciations occurred at the Oligocene-Miocene boundary leading then to the middle
5 Miocene Climatic optimum, and after to the Middle Miocene cooling (Keller et al., 1987;
6 Miller et al., 1991; Spezzaferri, 1995; Zachos et al, 1997, 2001 and 2008; Boulila et al.,
7 2011).

8 However, a paleoecological study on planktonic organisms requires an understanding of
9 how these water masses interact today with the living organisms, in terms of nutrients,
10 temperature and seasonal productivity.

11 1.2 Modern North Atlantic

12 At the present day the North Atlantic shows high biological productivity, owing to
13 nutrient-rich deep waters and winter mixing. This process renovates nutrient
14 concentration in surface waters, favouring the winter-spring plankton bloom. This is
15 followed by a strong vertical stratification during the summer, established by freshwater
16 additions and the warming of superficial layers. Tides can enhance the vertical mixing,
17 amplified by local effects, and further stimulating nutrient fluxes, to promote higher levels
18 of plankton production. All these processes affect planktonic foraminiferal assemblages,
19 influencing their latitudinal distribution (Townsend et al., 2004). Also, the dynamics of
20 the North Atlantic subpolar and subtropical gyres strongly determine the main features of
21 this region, where the major current systems include the Labrador Current and the North
22 Wall of the Gulf Stream. The Labrador Current is a cold, low salinity coastal current
23 originating on the west coast of Greenland from glacial melting (Chapman and Beardsley,
24 1989). At the Davis Strait (Greenland - Baffin Island) this current splits with one branch
25 flowing north into Baffin Bay, and the other crossing Davis Strait, where the West

1 Greenland Current, the Baffin Land Current (Baffin Bay) and Hudson Bay waters
2 (Hudson Strait) merge. This broad current extends from the continental shelf over the
3 continental slope and rise, and is commonly known as Labrador Slope Water. It continues
4 to flow south before subdividing again into two currents, mostly flowing along the outer
5 edge of the Grand Banks (Chapman and Beardsley, 1989). A continuous equatorward
6 coastal current system extends from Newfoundland south to the Middle Atlantic Bight,
7 which interacts with slope waters north of the Grand Banks, and the Gulf Stream.
8 The northwest Atlantic continental shelf waters can therefore be subdivided into multiple
9 regional systems, all interconnected to some extent to an equatorward-flowing coastal
10 current that has its origins in the Labrador Sea shelf. Within this context, shelf and slope
11 waters mix in complex ways both at surface and depth, and can be very important in
12 setting levels of primary production (Townsend et al., 2004). All these processes strongly
13 affected the amount of biogenic sedimentation (calcareous and siliceous micro and
14 nannofossils) during the last million years. Miller and Fairbanks (1983) suggested how
15 isotopic data from North Atlantic and eastern Pacific Ocean evidenced the similarity of
16 the late Oligocene – middle Miocene oceanic circulation of the western North Atlantic to
17 the present configuration.

18 2. Materials and Methods

19 This study is based on the analysis of 53 samples from the IODP-Hole U1406A (J-
20 Anomaly Ridge, 40°21'N, 51°39'W; Figure 1), belonging to the lithological Unit II - a
21 180 m thick Oligo-Miocene nannofossil ooze (Norris et al., 2014). Following van Peer et
22 al. (2017) the core composite depth below seafloor scale has been adopted. Thus, the
23 samples span from 96 to 23.4 m. Above this interval a reworked Miocene-Pleistocene
24 calcareous plankton assemblage has been recorded (Fabbrini et al., 2019), preventing a
25 reliable biostratigraphic interpretation. Fabbrini et al. (2019) also reported two hiatuses
26 in the upper portion of IODP-Hole U1406A. The most relevant at 38.85 m (2.10 Ma long)

1 and another one at 34.05 m (inferred 0.6 Ma long). The lowest hiatus involves the Biozone
2 M2-M3 limit and thus the Aquitanian-Burdigalian boundary. The total investigated
3 interval was constrained between Biozone O7 and M3 (Wade et al., 2011). For simplicity,
4 samples are indicated in terms of their depth expressed in metres from the seafloor.

5 2.1 Sample preparation and analysis setup

6 Sediment samples (10 cc in volume) were oven dried at 40° C and their dry weight
7 measured. Thereafter, the samples were soaked in distilled water and then washed through
8 a 63 µm sieve. This is the same dataset used for a biostratigraphic study published by the
9 authors (Fabbrini et al., 2019). For this study 53 samples were used and treated
10 statistically. The original foraminifera census data were collected counting 300 specimens
11 per sample on the fraction >125 µm. Each sample was observed under the
12 stereomicroscope, picking the planktonic foraminifera tests and glueing them onto
13 microslides, where species level identification was conducted, mainly referring to the
14 Atlas of Oligocene planktonic foraminifera (Wade et al., 2018). Before performing the
15 statistical analyses, each species was assigned to an ecogroup, mainly following Aze et
16 al. (2011), while the geographic distribution was based on Wade et al. (2018) and Schiebel
17 and Hemleben (2017).

18 The ecogroups indicate specific environmental conditions, based on the calcification
19 depth, capturing different water temperatures, upwelling conditions and nutrient supply
20 (Table 1). The environmental factors are all closely linked together, creating dynamic
21 ecosystems. For this reason, we decided to measure the abundance (relative percentage
22 in respect to the total of counted individuals per sample) of each ecogroup to evaluate
23 their reciprocal interactions. In parallel, we studied the behavior of each species using
24 multivariate analyses as a first screening tool. A final paleoclimatic model was created
25 combining all these results and data.

1 2.2 Statistical methods

2 We converted the census data of planktonic foraminifera in relative percentages. The
3 statistical analyses were performed using the paleontological software PAST-
4 Paleontological Statystic-ver 3.18 (Hammer, 2017). The statistical methods employed
5 were multivariate ordination analyses, in order to characterize the variations hidden in the
6 fossil assemblage and in the dataset. For this purpose, R-mode cluster analysis
7 investigated the components of the dataset and its spatial distribution. Principal
8 Component Analysis (PCA) was used to describe the reciprocal behavior of each species
9 in the assemblage. We followed the same methodology applied by Antonarakou et al.
10 (2007) to set up the data for the analyses. Species with abundance $< 1\%$ and belonging to
11 the same ecogroup were summed together to avoid background noise. With respect to the
12 original data set from Fabbrini et al. (2019), all samples with less than 250 counted
13 specimens were excluded indicating intervals affected by dissolution at the sea floor.
14 Fossil preservation was indicated by Benthos/Plankton and Fragments/Plankton ratios
15 (Fabbrini et al., 2019). In fact, high values of both these indicators highlight intervals
16 affected by strong chemical dissolution, indicating ocean floor acidification or oscillating
17 CCD.

18 Preliminary statistical screening allowed the identification of the maximum similarity
19 between samples in terms of their counted fossil assemblage. R-mode cluster analysis
20 allowed the characterization of the assemblages.

21

22 2.3 Paleoclimatic model (Shallow Dwellers Paleoclimatic Curve/SDPC)

23 The paleoclimatic model was created in two phases: after the recognition of three of the
24 ecogroups identified by Aze et al. (2011), we investigated the local behavior of these taxa
25 using multivariate and ordination analyses, identifying the most sensitive taxa in this
26 assemblage. Such taxa were finally plotted in a Shallow Dwelling Paleoclimatic Curve

1 (SDPC). This curve was created modifying the method described by Cita et al. (1977),
2 who proposed for the first time a single curve based on Pleistocene planktonic
3 foraminifera to pinpoint paleoclimatic variations. Cita et al., (1977) discriminated
4 planktonic foraminifera in latitudinal terms of warm, warm-temperate, cool-temperate,
5 cool and upwelling indices. Today, isotopic studies allow planktonic foraminifera to be
6 separated into ecogroups according to habitat and geographic distribution (Mortyn et al.,
7 2003 among the others).

8 In order to describe the ocean-atmosphere interaction and to represent a more reliable
9 surface water temperature model we used only species living in the mixed layer
10 (Ecogroup 1). Thus, only species belonging to Ecogroup 1 were employed to trace the
11 SDPC curve. Following literature and our statistical analysis, species were weighted
12 positively if having a warm water and oligotrophic affinity and negatively if possessing
13 cold water and eutrophic affinity. Thus, the SDPC was constructed as the sum of positive
14 taxa (warm taxa living in the open ocean mixed layer) and negative taxa (cold taxa of the
15 open ocean mixed layer).

16 3. Results and Discussion

17 3.1 Ecogroups division

18 Following Aze et al. (2011), the ecogroups recognized in this assemblage are three:
19 Ecogroup 1- open ocean mixed layer, Ecogroup 3 – thermocline, Ecogroup 4 –
20 subthermocline taxa (Table 1). No taxa belonging to Ecogroup 2 (Aze et al., 2011),
21 shallow dwelling taxa symbionts barren, are represented in this assemblage. In the
22 following paragraphs species sharing the same habitat and lifestyle are described together
23 as a group, while species needing special mention are described individually (even though
24 grouped together for analytical purposes).

25 Ecogroup 1

1 These taxa live and calcify their test in the open ocean mixed layer, where water
2 temperature is higher, CO₂ less abundant and trophic conditions are more dynamic. This
3 ecogroup favours warm-temperate water conditions, with a deep thermocline and thus a
4 thicker mixed layer due to stronger stratification of the water column. The isotopic ratios
5 of these taxa show the lowest δ¹⁸O and the highest δ¹³C values among all foraminifera,
6 with the high δ¹³C due to the presence of algal symbionts in their tests (Spezzaferri, 1995;
7 Aze et al., 2011; Schiebel and Hemleben, 2017). The components of this group (Table 1)
8 are: *Globigerina bulloides*, *Trilobatus* gr. (*T. immaturus*, *T. primordius*, *T. trilobus* and
9 *Globigerinoides subquadratus*), *Paragloborotalia kugleri* gr. (*P. kugleri* and *P.*
10 *pseudokugleri*), *Globoturborotalita* gr. (*G. connecta*, *G. occlusa*, *G.*
11 *pseudopraebulloides*).

12 *Globigerina bulloides* calcifies its test between 30-50 m depth (Spero and Lea, 1996;
13 Niebler et al., 1999) at equilibrium conditions, as indicated by its stable isotope ratios
14 (Curry and Matthews, 1981; Kahn and Williams, 1981; Deuser and Ross, 1989; Sautter
15 and Thunell, 1991; Spero and Lea, 1996). Aze et al. (2011) reported *G. bulloides* in
16 Ecogroup 2 as a symbiont-barren species, which was later confirmed by Schiebel and
17 Hemleben (2017) and by Spezzaferri et al. (2018). In addition, Aze et al. (2011) listed
18 another species (*G. praebulloides*) as a symbiont bearing species (Ecogroup 1) in
19 specimens from the Oligocene-Miocene transition in Ceara Rise (Pearson et al., 1997).
20 *Globigerina praebulloides* was then synonymized with *Globigerenella obesa* in
21 Spezzaferri et al. (2018), thus specimens previously identified as *G. praebulloides* were
22 reassigned as *G. bulloides* and as *Globoturborotalita pseudopraebulloides* when
23 presenting a cancellate wall texture. However, no pictures were provided of *G.*
24 *praebulloides* specimens in Pearson et al. (1997) preventing their identification as *G.*
25 *bulloides* or as *G. pseudopraebulloides*. Moreover, very little information is available

1 about the paleoecology of *G. bulloides* in the earliest Miocene, leading us to assign our
2 *G. bulloides* to Ecogroup 1 instead of to Ecogroup 2.

3 *Trilobatus immaturus*, *T. primordius*, *T. trilobus* and *Globigerinoides subquadratus* are
4 grouped together because they show similar isotopic ratios typical of the open ocean
5 mixed layer habitat in warm and warm-temperate waters. This group is rare or absent in
6 areas of strong upwelling conditions (Kennett and Srinivasan, 1983; Spezzaferri, 1995).

7 *Paragloborotalia kugleri* and its ancestor *P. pseudokugleri* both show very light $\delta^{18}\text{O}$
8 ratio indicating a superficial habitat. These taxa favoured high productivity water
9 (eutrophic conditions) especially at low and mid latitudes (Leckie et al., 2018, among
10 others).

11 In the *Globoturborotalita* group, *G. ouachitaensis* is reported in the mixed layer by
12 Sexton et al. (2006), and is indicated by Pearson and Wade (2009) during the Eocene as
13 a shallow and warm taxon, due to negative $\delta^{18}\text{O}$ values. *Globoturborotalita connecta* and
14 *G. woodi* are reported by Spezzaferri et al. (2018) as shallow dwellers, falling with the
15 others in the *Globoturborotalita* group.

16 Ecogroup 3

17 This group lives between the dynamic superficial water layers and the colder and denser
18 water below the thermocline, thus it shows higher values of $\delta^{18}\text{O}$ and lower values of $\delta^{13}\text{C}$
19 than Ecogroup 1. This group comprises (Table 1): *Dentoglobigerina larmei* gr. (*D.*
20 *larmei*, *D. baroemouensis*, *D. globularis*, *Globoquadrina dehiscens*), *Globigerinella*
21 (*Globigerinella obesa*), *Tenuitella* group. (*Tenuitella angustiumbilitata*, *T. munda*),
22 *Paragloborotalia* group (*P. acrostoma*, *P. nana*, *P. siakensis*, *P. semivera*) and
23 *Sphaeroidinellopsis disjuncta*.

24 *Globigerinella obesa* is a thermocline species abundant in tropical and warm-temperate
25 conditions (Spezzaferri, 2002), and also the tenuitellids (according to Pearson et al., 2018,

1 *Tenuitella* and *Tenuitellinata* belong to the same genus (*Tenuitella*) prefer warm habitats
2 (Pearson, 1997; Pearson and Wade, 2009). *Paragloborotalia acrostoma* is considered a
3 warm/warm-temperate species by Spezzaferri (2002), while *Paragloborotalia siakensis*
4 and *P. semivera* are typical of warm conditions, but with isotopic ratios indicating they
5 are upper thermocline dwellers (Pearson and Wade, 2009; Leckie et al., 2018).
6 *Paragloborotalia nana* had an upper thermocline habitat as well, even though
7 documented also at high latitudes (Matsui et al., 2016; Leckie et al., 2018).
8 *Globoquadrina dehiscens* is considered a cosmopolitan species with an erratic and
9 variable lifestyle (Pearson and Shackleton, 1995), but it is reported as an intermediate
10 dweller by Keller et al. (1985). In this paper, this taxon is considered as a thermocline
11 inhabitant (Table 1), following Aze et al. (2011), and grouped together with its ancestor
12 *Dentoglobigerina larmei*, another thermocline inhabitant (Pearson and Wade, 2009;
13 Wade et al., 2018).
14 *Sphaeroidinellopsis disjuncta* is most likely a descendant of *G. woodi* (Kennett and
15 Srinivasan, 1983) and stable isotope data classify it as a thermocline calcifier (Aze et al.,
16 2011), especially abundant at low latitudes and during warm and temperate conditions
17 (Kennett and Srinivasan, 1983).

18 Ecogroup 4

19 In previous literature, these taxa are sometimes referred to as “deep dwellers”, because
20 their life cycle occurs mostly below the thermocline. These taxa are characterized by the
21 highest values of $\delta^{18}\text{O}$ and the lowest of $\delta^{13}\text{C}$ (Poore and Matthews, 1984; Spezzaferri,
22 1995; Aze et al., 2011; Schiebel et al., 2017 and references therein). Higher abundance of
23 these taxa indicates a thinner mixed-layer and thus a more superficial thermocline (Ravelo
24 and Fairbank, 1990; Kennett et al., 1985). In fact, where the thermocline is more
25 superficial the habitat for these taxa is wider allowing them to proliferate. As summarised
26 in Table 1, the components of this group are: *Catapsydrax* gr. (*C. dissimilis*, *C. unicavus*),

1 *Dentoglobigerina venezuelana* gr. (*D. binaiensis*, *D. tripartita*, *D. venezuelana*),
2 *Globorotalia* gr. (*G. praescitula*, *G. miozea*), *Globorotaloides* gr. (*G. stainforthi*, *G.*
3 *suteri*). *Catapsydrax* gr. and *Globorotaloides* gr. have the highest $\delta^{18}\text{O}$ values (Poore and
4 Matthews, 1984; Coxall and Spezzaferri, 2018) indicating a superficial thermocline or
5 strong upwelling conditions. *Dentoglobigerina tripartita* is a cosmopolitan species, but a
6 change in its habitat was documented in the early Oligocene (van Eijden et al., 1995).
7 Stewart et al. (2012) reported *D. venezuelana* as a deep dweller during the adult stage,
8 while it is reported as a thermocline dweller by Si et al. (2018). No consensus exists on
9 the habitat of different morphotypes (adult or pre-adult calcification stage) leading to
10 uncertain isotopic analyses (Gasperi and Kennett, 1993; Pearson and Shackleton, 1995;
11 Pearson et al., 1997; Pearson and Wade, 2009; Nathan and Leckie, 2009; Aze et al., 2011;
12 Stewart et al., 2012; Si et al., 2018). For these reasons, we distinguished no morphotypes
13 in this study, considering *D. venezuelana* as a morphologically variable taxon (Table 1).
14 *Globorotalia praescitula* is the ancestor of *Gl. miozea*, indeed the specimens here
15 identified as *Gl. miozea* show intermediate features between the two taxa. Thus, *Gl.*
16 *miozea* is here grouped together with *Gl. praescitula* in Ecogroup 4 as a subthermocline
17 dweller. *Gl. praescitula* is reported as a temperate to tropical species by Kennett and
18 Srinivasan (1983) and low to middle latitudes by Aze et al. (2011).

19 3.2 Cluster analysis

20 Hierarchical cluster analysis allowed us to pinpoint different distribution and preferential
21 patterns in the fossil assemblage. The cophenetic correlation index result was 0.82 for R-
22 mode with the Euclidean distance, indicating good reliability (Coph.corr. >0.75). Cutting
23 at 0.3 similarity value (Figure 2) the R-mode analysis identified two main clusters (A and
24 B in Figure 2) and an out-group formed by *Globigerinella* gr. (the taxon is rare but
25 regularly distributed along the entire section). Cluster A is composed of *Globorotalia* gr.,
26 *S. disjuncta* and *Trilobatus* gr., which is clearly determined by the different spatial

1 distribution of these taxa. In fact, taxa grouped in Cluster A reach their abundance peak
2 in the upper portion of the section. The presence of *Globorotalia* gr. and *S. disjuncta* can
3 be linked to their first appearance in the fossil record that occurred during the time interval
4 of the hiatus H1 (Fabbrini et al., 2019). Cluster B comprises two elements. The first one
5 is *Globigerinita glutinata* and the second is a subcluster made of *Catapsydrax* gr., *D.*
6 *larmei* gr., *D. venezuelana* gr., *G. bulloides* gr., *Globorotaloides* gr., *Globoturborotalita*
7 *gr.*, *Paragloborotalia* gr., *P. kugleri* gr., *Tenuitella* gr. As shown in Figure 2,
8 *Globigerinita glutinata* contrasts all the other members of cluster B, suggesting a different
9 distribution with respect to all the other taxa. In fact, *G. glutinata* is the dominant species
10 of the fossil assemblage. Similar behaviors occur inside cluster B for taxa belonging to
11 the same ecogroup, such as *Catapsydrax* gr. and *Globorotaloides* gr., *Globigerina*
12 *bulloides* and *Globoturborotalita* gr.

13 3.3 Principal Component Analysis (PCA)

14 The ordination analysis allowed the behavior of apparently similar taxa to be clarified
15 (Figure 3). The PCA plot indicates clearly the predominance of *Globigerinita glutinata*,
16 which is weighted positively in terms of the PC1 and therefore significantly different from
17 all the other taxa. This analysis also pinpoints the different distribution of
18 *Paragloborotalia* gr. with respect to the other taxa.

19 In fact, *Paragloborotalia* gr. is weighted positively for PC1 and PC2, but PC2 influences
20 the distribution of this group. *Paragloborotalia* gr. species belong to Ecogroup 3 (Aze et
21 al., 2011 and Leckie et al., 2018) and were common in tropical to subtropical waters,
22 especially in tropical upwelling areas as are some modern *Neogloboquadrina* (Leckie et
23 al., 2018).

24 *Globigerinita glutinata*, still living today, is reported as an opportunistic species
25 belonging to Ecogroup 1 (Schiebel and Hemleben, 2017) inhabiting the uppermost mixed

1 layer (water depth < 75 metres). It is a cosmopolitan species spreading within a wide
2 range of temperature and salinity, which can survive both in oligotrophic and eutrophic
3 conditions (Hemleben et al., 1989, Mazumder et al., 2009). Sometimes its presence is
4 associated with the spring bloom, triggered by newly available nutrients at the end of the
5 winter mixing and increased solar irradiation (Casford et al., 2002). According to
6 Schiebel et al. (2017) *G. glutinata* decreases in abundance from low to high latitudes. It
7 can be transported to subpolar or polar areas becoming dominant in the assemblage during
8 the summer. At lower latitudes *G. glutinata* blooms are linked to nutrients and food
9 production at the depth of the seasonal thermocline (Schiebel et al., 2001). Stangeew
10 (2001) documented *G. glutinata* as the major constituent of the foraminiferal summer
11 assemblage in the Labrador Sea (south of Greenland).

12 *Globigerina bulloides* is weighted positively for both principal components. Thus, it is
13 closely related to *G. glutinata*, belonging to Ecogroup 1. *Globigerina bulloides* inhabits
14 the mixed layer withstanding large fluctuations in temperature, salinity and density of the
15 water column. This species is more abundant in high productivity environments and is
16 influenced by upwelling conditions, strong seasonal mixing and fresh water inputs
17 (Rohling et al., 1993).

18 *Globoturborotalita* gr. is weighted negatively for PC1 as opposed to *G. bulloides*. Both
19 belong to the same Ecogroup 1, but have different climatic affinity. *Globoturborotalita*
20 gr. inhabited preferentially warm waters at low and mid latitudes. In this group, *G.*
21 *pseudopraebulloides* and *G. occlusa* were widespread and abundant, while *G. connecta*
22 was cosmopolitan but generally rare.

23 *Trilobatus* gr. and *Paragloborotalia kugleri* gr. (*P. kugleri* and *P. pseudokugleri*) are
24 weighted negatively in terms of PC1 and PC2, which is completely opposite to *G.*
25 *bulloides*. These two groups inhabited the warm water of the mixed layer as suggested by

1 their isotopic signature. They were global taxa preferring warmer conditions at low and
2 middle latitudes.

3 *Trilobatus* gr. (and *Globigerinoides*) are oligotrophic taxa typical of well stratified water
4 masses, absent or very rare in upwelling regions (Spezzaferrri et al., 2018 and references
5 therein), where oceanic currents mix the water masses creating eutrophic conditions, and
6 high primary productivity and algal blooms. Thus, *Trilobatus* gr. indicates warm and
7 strongly stratified water columns. The stratification of the water column is the main
8 controlling factor of the distribution of this group (Rohling et al., 1997). Living taxa such
9 as *Globigerinoides ruber* and *Trilobatus sacculifer* live close to the surface preferring low
10 nutrient conditions during summer months in areas where the solar radiation is highest
11 (Hemleben et al., 1989).

12 *Paragloborotalia kugleri* gr. favoured eutrophic conditions mostly in tropical to
13 subtropical environments (Leckie et al., 2018 and references therein). Pearson and Wade
14 (2009) suggested a symbiotic association in *P. pseudokugleri* based on stable isotope data.
15 This group preferred eutrophic conditions in temperate to high latitude waters.

16 All taxa belonging Ecogroup 4 are weighted negatively for the PC1 as opposed to *G.*
17 *glutinata*, *G. bulloides* and *Paragloborotalia* gr. (Figure 3). At a closer look interesting
18 details emerge, *Catapsydrax* gr. and *Globorotaloides* gr. are weighted differently for PC2,
19 even though they have similar isotopic signatures, typical of subthermocline habitats and
20 both showed affinities to high productivity conditions. In fact, *Catapsydrax* gr. was
21 global, especially common at high latitudes and in upwelling regions. *Globorotaloides*
22 gr. was global, but more common in low and mid latitudes. *Globorotalia* gr. is weighted
23 very similar to *Globorotaloides* gr. The living *G. scitula* is the descendant of *G.*
24 *praescitula* and is associated with cool water conditions (Rohling et al., 1993). Other

1 living taxa such as *Globorotalia crassaformis* inhabit a subthermocline habitat in
2 equatorial areas and superficial waters at polar/subpolar latitudes (Schiebel et al., 2017).

3 *Dentoglobigerina venezuelana* gr. are weighted the same as *Catapsydrax* gr. In fact, their
4 isotopic signatures indicate deep water habitats, even if some authors documented
5 shallower habitats (Poore and Matthews, 1984; Wade et al., 2007; Beltran et al., 2014;
6 Moore et al., 2014). These taxa might have changed habitat during their life cycle,
7 migrating to deep water in the adult stage (Wade et al., 2018). They were global but
8 particularly abundant at low and mid latitudes.

9 Taxa belonging to Ecogroup 3 are weighted negatively for both the PC, sharing
10 similarities with taxa of Ecogroup 1 and 4 (Figure 3). Thermocline dwellers show
11 intermediate isotopic signatures with respect to other ecogroups (Aze et al., 2011 among
12 others), inhabiting the thermocline level they may be more tolerant to latitudinal and
13 thermal variability.

14 *Dentoglobigerina larmeyi* was cosmopolitan; even recorded at polar latitudes at DSDP
15 Site 407 (Poore, 1979). Pearson and Wade (2009) and Aze et al. (2011) proposed an upper
16 thermocline habitat based on isotopic signature. *D. globularis* was widespread in low to
17 mid-latitudes. Biolzi (1983) suggested a mixed-layer habitat but the species was not
18 illustrated preventing a reliable identification. Wade et al. (2007) showed variable
19 isotopic ratios, but Aze et al. (2011) classified this taxon in Ecogroup 3. *Globoquadrina*
20 *dehiscens* was also cosmopolitan and classified as an intermediate-dweller by Keller
21 (1985). Pearson and Shackleton (1995) suggested this species as erratic and variable; it is
22 located in Ecogroup 3 by Aze et al. (2011).

23 *Tenuitella* gr. was not reported in Aze et al. (2011) but is described in Pearson et al. (2018)
24 as an inhabitant of the warm surface mixed-layer, following suggestions by earlier authors
25 (Poore and Matthews, 1984; van Eijden and Ganssen, 1995; Pearson et al., 1997; Pearson

1 and Wade, 2009). *Tenuitella* was documented from the tropics to high latitudes.
2 *Globigerinella* gr. is reported by Aze et al. (2011) in Ecogroup 3 at thermocline depth.
3 These taxa are documented from low to mid latitudes and are, particularly abundant in
4 oligotrophic tropical areas (Spezzaferri et al., 2018). Even if *Globigerinella siphonifera*
5 today inhabits the mixed layer and is a symbiont-bearing species, it is not known if it has
6 changed habitat with respect to its ancestral taxon (*G. praesiphonifera*) or if the carbon
7 isotope offset is a vital effect.

8 *Sphaeroidinellopsis disjuncta* is shown in Ecogroup 3 as a thermocline dweller by Aze et
9 al. (2011) and inhabited mostly low latitudes (Kennett and Srinivasan, 1983). PCA
10 analysis therefore allowed species with contrasting behavior, such as *Globoturborotalita*
11 gr. and *G. bulloides* and *Trilobatus* gr., to be separated (Figure 3).

12 3.4 Ecogroups distribution and paleoclimatic observations

13 We plotted the distribution of the ecogroups vs. depth/magnetostratigraphy to infer the
14 changes occurring in the water column and the stratification of changing foraminiferal
15 habitats. Three curves (Figure 4) were produced summing together the census values of
16 all the species belonging to the same ecogroup (Table 1). These curves enable reciprocal
17 behavior of these groups to be compared. The curves indicate clearly that ecological
18 variations occurred. In fact, the mixed-layer dweller curve (Ecogroup 1) and the deep
19 dwelling taxa curve are in opposition (Ecogroup 4), suggesting a reciprocal influence
20 between the habitats. All the shallow dwellers minima correspond to deep dwellers
21 maxima (Figure 4). On the other hand, the intermediate dweller curve (Ecogroup 3)
22 depicts more complex behavior. At some points they mirror the shallow dweller taxa and
23 in other points they resemble the deep dwellers. This ambivalent behavior could be linked
24 either to real intermediate habitat conditions or to misinterpretation of some taxa. Higher
25 abundance of Ecogroup 1 can be related to a mixed-layer expansion allowing superficial

1 taxa to proliferate. The vertical expansion of the mixed-layer might be induced by
2 multiple factors. Increased supply of warmer superficial water masses from the North
3 Wall Gulf Current could cause the expansion of the superficial mixed layer and deepening
4 of the thermocline.

5 The relationship between thermocline fluctuations and SST (sea surface temperature)
6 were investigated tracing the SDPC (Figure 4). We traced this curve based on the climatic
7 curve published by Cita et al. (1977). Instead of using all taxa, we took into consideration
8 only taxa from Ecogroup 1, as direct and more reliable indicators of the surface water
9 conditions. The curve depicts higher superficial temperature when positive and lower
10 temperatures when values are negative or decrease. Thus, the SDPC shows the
11 relationship between 1) *Trilobatus* gr., *Globoturborotalita* gr., *Paragloborotalia kugleri*
12 gr. and 2) *Globigerina bulloides*. The SDPC shows great variability along the section,
13 highlighting some intervals with negative values or strong decreases. The negative
14 intervals at 87 m, 85 m, 58-56 m, 45-42 m, 32-30 m, 29-26 m, 25-24 m represent
15 dominance of *G. bulloides* over other mixed layer taxa. This dominance could be
16 associated with increased primary productivity in eutrophic conditions. A stronger
17 influence of colder water masses of the Labrador Current and even increased upwelling
18 conditions possibly induced *G. bulloides* to proliferate. Thus, all the negative peaks may
19 be linked to stadial events or colder and more productive superficial water.

20 Higher species diversity is often linked to warmer conditions or interstadial conditions
21 and is generally higher at low and mid latitudes rather than at polar/subpolar latitudes.
22 The Shannon Index describes the species diversity and it can be used to evaluate the
23 richness of the fossil assemblages.

24 In Figure 4 the two curves are plotted together showing a similar trend. The general
25 accordance between the two curves supports the connection between superficial water

1 temperature and species diversity. A secondary observation can be made using
2 radiolarians, which are abundant along the entire section (Norris et al., 2014), reaching
3 their maximum abundance at two intervals (Figure 4). Both these intervals coincide with
4 a fall of the SPDC. Radiolarians can be considered an indicator of cold waters, especially
5 abundant at polar/subpolar latitudes, even though at 56 m their abundance can be
6 attributed to higher dissolution rate as shown by F/P and B/P curves (Figure 4).

7 The IODP Site U1406 was drilled at 3800 m water depth and its paleobathymetry is
8 exstimated at 3500 m in the early Miocene (Norris et al., 2014), making it vulnerable to
9 CCD oscillations. The B/P ratio (Benthic foraminifera/ Planktonic foraminifera) and F/P
10 (planktonic fragments/planktonic foraminifera) are plotted here for comparison to
11 evaluate the fossil preservation. High values of the two parameters suggest poor
12 preservation due to chemical dissolution of foraminiferal tests, such as in four intervals:
13 77 -75 m, 67 - 65 m, 61 - 59m and 38-34 m. The SDPC appears poorly related to B/P and
14 F/P, suggesting limited influence of chemical dissolution on the SDPC curve, which
15 presumably describes genuine climatic variations.

16 The studied section contains two hiatuses as described by Fabbrini et al. (2019), at 38.85
17 m and at 34.05 m (indicated with dashed lines in Figure 4). Even if the two hiatuses have
18 been well biostratigraphically constrained, we preferred to cut the paleoclimatic model at
19 hiatus 1 (38.85 m) in order to avoid misleading interpretations.

20 In Figure 5 the final model is plotted against time. Using the age model provided by
21 Fabbrini et al. (2019) the interval studied spans from 23.50 Ma to 21.25 Ma. The SDPC
22 and Shannon Index curve have been smoothed for a direct comparison with the two other
23 curves from literature: 1) the $\delta^{18}\text{O}$ stack from the North Atlantic (Cramer et al., 2009) and
24 2) the SST-Alkenone from IODP Site U1404 (Liu et al., 2018) using chemical data to
25 reconstruct deep water temperature (from benthic foraminifera) and the superficial water

1 temperature (SST), respectively. The $\delta^{18}\text{O}$ shows smoother oscillations with three
2 minima, around 22.75 Ma and around 22 Ma and at 21.25 Ma. Then it shows three
3 maxima points, at 23.30 Ma, around 22.40 Ma and around 21.60 Ma. The SST curve
4 depicts more oscillations with five negative peaks and four main positive peaks. The
5 temperature minimum is documented at 22.50 Ma, which corresponds to rising values of
6 the $\delta^{18}\text{O}$ stack. From 22 Ma upwards a good accordance among the two curves can be
7 observed. The SDPC shows a generally good match with the $\delta^{18}\text{O}$, but a greater similarity
8 to the Alkenone SST. In fact, until 23 Ma all the curves indicate a gradual lowering of the
9 temperatures, suggesting a general cooling of the superficial water mass. At 23 Ma
10 Boulila et al. (2011), among the others, documented the Megahiatius Mi1 affecting the
11 North Atlantic and potentially recognizable at global scale. Boulila et al. (2011) suggested
12 a connection between such megahiatius and the obliquity node at 22.98 Ma of long-period
13 (~ 1.2 Ma) obliquity cycles as recognizable in the obliquity variation curve in Laskar et
14 al. (2004). Following Miller et al. (1985), the megahiatius Mi1 occurs between the 3rd
15 order sequence O7 and KW0 of the New Jersey seashelf, and encompasses the
16 Oligocene/Miocene boundary. Megahiatius Mi1 is not documented in IODP Hole
17 U1406A but a climatic signal corresponding to the general oceanic cooling is clearly
18 recorded by planktonic foraminifera and thus evident in the SDPC. At the end of the Mi1
19 event another SDPC drop occurs, coinciding with $\delta^{18}\text{O}$ and SST low values. The SDPC
20 also captures the same climatic improvement described by the SST warming, maybe
21 linked to a short interstadial event around 22.80 Ma and not documented by the $\delta^{18}\text{O}$ data.
22 Around 22.60 Ma all three curves indicate rising temperature, first recorded by the SST-
23 Alkenone and by the SDPC and slightly later by the $\delta^{18}\text{O}$, further supporting the
24 successful correlation of the SDPC with the Alkenone-SST. At 22.50 Ma the SDPC and
25 SST document a drastic fall of the superficial temperature and thus a strengthening of the

1 Labrador current. This SST minima is not recorded by the $\delta^{18}\text{O}$, which in contrast suggest
2 higher temperature at the ocean floor.

3 The interval between 22.50 -22 Ma seems to show no correspondence among the SDPC
4 and SST. In fact, while the $\delta^{18}\text{O}$ data show a temperature peak, perfectly mirrored by the
5 SDPC (22.50-22.25 Ma), the SST shows a continuously rising trend. However, in this
6 interval, the situation depicted by Alkenone data could partially represent the temperature
7 oscillations at the J-Anomaly Ridge. In fact, in this interval, the SST curve is based on
8 two sample-level only (22.40 Ma and at 22.05 Ma in Liu et al., 2018). The SST peak at
9 21.99 Ma is evident in the smoothed SDPC, where the Shannon Index mirrors the $\delta^{18}\text{O}$
10 stack. Then all the curves fall coinciding with the temperature minimum recorded by the
11 $\delta^{18}\text{O}$ stack. At this age the Earth was in another nodal position (Laskar et al., 2004) and
12 thus another megahiatus is documented in the North Atlantic by Boulila et al. (2011). The
13 megahiatus linked to the “unnamed” event spans from 21.99 Ma to 21.20 Ma, but is not
14 documented in IODP Hole U1406A. Around 21.60 Ma the high values of the $\delta^{18}\text{O}$ is
15 documented also by a maximum in the SDPC. In this time frame the SST-Alkenone from
16 Liu et al (2018) is affected by low sample resolution, thus not giving a complete record
17 of the temperature variations. The SST peaks at 21.40 Ma, while $\delta^{18}\text{O}$ and the SDPC are
18 decreasing. At 21.30 Ma another minimum occurs in SDPC and SST, during the steady
19 lowering trend of the $\delta^{18}\text{O}$ stack. In correspondence with Hiatus 1 (38.85 m, in Fabbrini
20 et al., 2019) SDPC and SST increase rapidly, in contrast with the $\delta^{18}\text{O}$ data. Thus, Hiatus
21 1 is not directly linked to any regional megahiatus and occurred at the end of the
22 “unnamed” glacial event.4.

23 Conclusions

24 The planktonic foraminifera quantitative distribution from IODP Hole U1406A reveal
25 intriguing information about the paleoclimatic changes occurring in the North Atlantic

1 Ocean during the uppermost Oligocene-lower Miocene interval. Following Aze et al.
2 (2011), three foraminiferal ecogroups are recognized: Ecogroup 1- open ocean mixed
3 layer with symbionts, Ecogroup 3 – thermocline, Ecogroup 4 – subthermocline taxa.
4 Results from statistical analyses suggest that Ecogroup 1 is the most suitable in
5 reconstructing the sea surface variations, and among the superficial water taxa,
6 *Globigerina bulloides*, *Globoturborotalita* gr. and *Trilobatus* gr. are the most sensitive to
7 environmental factors, such as superficial water temperature and trophic conditions. The
8 Shallow Dwellers Paleoclimatic Curve (SDPC) presented in this paper, accurately mirror
9 the SST-Alkenone data from the Site U1404 (Liu et al., 2018) and the $\delta^{18}\text{O}$ stack (Cramer
10 et al., 2009). The Shannon-Weaver index also tends to mirror primarily the $\delta^{18}\text{O}$ stack
11 and secondly the SST curve. The SDPC and the Shannon-Weaver index curve
12 significantly drop in correspondence of the “Mi1” and “Unnamed” events reported by
13 Boulila et al. (2011), indicating colder water conditions. Those events are visible at 22.90-
14 22.80 Ma and at 21.95-21.90 Ma respectively, perfectly fitting with the obliquity nodes
15 of the Earth (Laskar et al., 2004). These relationships support the use of open ocean
16 mixed-layer (Ecogroup 1) planktonic foraminifera as sensitive indicators of SST,
17 particularly where isotopic data are not available. The taxa living in the mixed-layer
18 showed a close relation with the other taxa living in deeper levels of the water column,
19 due to the connection of their habitats. In fact, the taxa living in the open ocean mixed
20 layer always present an opposite trend to the subthermocline dwelling taxa, while the
21 thermocline dwellers show intermediate features and seem more tolerant to ecological
22 variations. This multi-approach study confirms the utility of the taxa inhabiting the open
23 ocean mixed layer to document sea surface temperature and some ecological variations.
24 Paleoecological data fit really well with geochemical data and pinpoint the dynamic
25 balance between the ecogroups and their habitat.

1 Acknowledgements

2 We are very thankful to Paul Minton for the linguistic revision of the manuscript. We
3 would like also to thank the three reviewers and the editor for their helpful comments and
4 contributions.

5 References

- 6 Antonarakou A, Drinia H, Tsaparas N, Dermitzakis MD (2007). Micropaleontological
7 parameters as proxies of late Miocene surface water properties and paleoclimate in
8 Gavdos Island, eastern Mediterranean. *Geodiversitas*, 29 (3): 379-99.
- 9 Aze T, Ezard TH, Purvis A, Coxall HK, Stewart DR et al. (2011) A phylogeny of
10 Cenozoic macroperforate planktonic foraminifera from fossil data. *Biological Reviews*,
11 86 (4): 900-27.
- 12 Beltran C, Rousselle G, Backman J, Wade BS, Sicre, M. A. (2014). Paleoenvironmental
13 conditions for the development of calcareous nannofossil acme during the late Miocene
14 in the eastern equatorial Pacific. *Paleoceanography*, 29 (3): 210-222.
- 15 Biolzi M (1983). Stable isotopic study of Oligocene-Miocene sediments from DSDP Site
16 354, equatorial Atlantic. *Marine Micropaleontology*, 1, 8 (2): 121-39.
- 17 Boulila SBS, Galbrun B, Miller KG, Pekar SF, Browning JV et al. (2011). On the origin
18 of Cenozoic and Mesozoic “third-order” eustatic sequences. *Earth-Science Reviews* 109:
19 94–112.
- 20 Boyle EA, Keigwin L (1987). North Atlantic thermohaline circulation during the past
21 20,000 years linked to high-latitude surface temperature. *Nature*, 330 (6143): 35.

1 Boyle PR, Romans BW, Tucholke BE, Norris RD, Swift SA et al. (2017). Cenozoic North
2 Atlantic deep circulation history recorded in contourite drifts, offshore Newfoundland,
3 Canada. *Marine Geology*, 1 (358): 185-203.

4 Broecker W (1997). Future directions of paleoclimate research. *Quaternary Science*
5 *Reviews*, 1, 16 (8), 821-5.

6 Brunner CA, Maniscalco R (1998). Late Pliocene and Quaternary paleoceanography of
7 the Canary Island region inferred from planktonic foraminifer assemblages of Site 953.
8 In: Weaver PPE, Schmincke HU, Firth JV, Duffield W (editors). *Proceedings of the*
9 *Ocean Drilling Program, Scientific Results, Vol. 157*, pp.73-82.

10 Casford JSL, Rohling EJ, Abu-Zied R, Cooke S, Fontanier C et al. (2002). Circulation
11 changes and nutrient concentrations in the late Quaternary Aegean Sea: a nonsteady state
12 concept for sapropel formation. *Paleoceanography and Paleoclimatology*, 17 (2).

13 Chapman DC, Beardsley RC (1989). On the origin of shelf water in the Middle Atlantic
14 Bight. *Journal of Physical Oceanography*, 19 (3): 384-391.

15 Cita MB, Vergnaud-Grazzini C, Robert C, Chamley H, Ciaranfi N et al. (1977).
16 Paleoclimatic record of a long deep sea core from the eastern Mediterranean. *Quaternary*
17 *Research*, 8 (2): 205-235.

18 Coxall HK, Spezzaferri S (2018). Taxonomy, biostratigraphy, and phylogeny of
19 Oligocene *Catapsydrax*, *Globorotaloides*, and *Protentelloides*. In: Wade BS, Olsson RK,
20 Pearson PN, Huber BT, Berggren WA (editors). *Atlas of Oligocene Planktonic*
21 *Foraminifera*, Cushman Foundation of Foraminiferal Research, Special Publication, No.
22 46, pp. 79-125.

1 Cramer BS, Toggweiler JR, Wright JD, Katz ME, Miller KG (2009). Ocean overturning
2 since the Late Cretaceous: Inferences from a new benthic foraminiferal isotope
3 compilation. *Paleoceanography and Paleoclimatology*, 24 (4).

4 Curry WB, Matthews RK (1981). Paleo-oceanographic utility of oxygen isotopic
5 measurements on planktic foraminifera: Indian Ocean core-top evidence.
6 *Palaeogeography, Palaeoclimatology, Palaeoecology*, 1, 33 (1-3):173-191.

7 Deuser WG, Ross E (1989). Seasonally abundant planktonic foraminifera of the Sargasso
8 Sea; succession, deep-water fluxes, isotopic compositions, and paleoceanographic
9 implications. *The Journal of Foraminiferal Research*, Oct. 1, 19 (4): 268-293.

10 Fabbrini A, Baldassini N, Caricchi C, Di Stefano A, Dinarès Turell J et al. (2019).
11 Integrated quantitative calcareous plankton bio-magnetostratigraphy of the Early
12 Miocene from IODP Leg 342, Hole U1406A (Newfoundland Ridge, NW Atlantic
13 Ocean). *Stratigraphy and Geological Correlation*, 27 (2): 259–276. DOI:
14 10.1134/S0869593819020023

15 Faugères JC, Stow DA, Imbert P, Viana A (1999). Seismic features diagnostic of
16 contourite drifts. *Marine Geology*, Dec 1, 162 (1): 1-38.

17 Gasperi JT, Kennett JP (1993). Vertical thermal structure evolution of Miocene surface
18 waters: western equatorial Pacific DSDP Site 289. *Marine Micropaleontology*, Oct 1, 22
19 (3): 235-54.

20 Hammer Ø(2017). The past and future of PAST—paleontological statistics software,
21 version 3.

22 Hemleben C, Spindler M, Erson OR (1989). *Modern planktonic foraminifera*. Springer,
23 Berlin.

- 1 Heezen BC, Hollister C (1964). Deep-sea current evidence from abyssal sediments.
2 Marine Geology, 1 (2): 141-74.
- 3 Heezen BC, Hollister CD, Ruddiman WF (1966). Shaping of the continental rise by deep
4 geostrophic contour currents. Science, 152 (3721): 502-8.
- 5 Kahn MI, Williams DF (1981). Oxygen and carbon isotopic composition of living
6 planktonic foraminifera from the northeast Pacific Ocean. Palaeogeography,
7 Palaeoclimatology, Palaeoecology, 33 (1-3): 47-69.
- 8 Keller G. (1985). Depth stratification of planktonic foraminifers in the Miocene ocean.
9 Geological Society of America Memoir, 163.
- 10 Keller G, Herbert T, Dorsey R, D'Hondt S, Johnsson M, Chi WR (1987). Global
11 distribution of late Paleogene hiatuses. Geology, 15 (3): 199-203.
- 12 Kennett JP, Srinivasan MS (1983). Neogene planktonic foraminifera: a phylogenetic
13 atlas. Hutchinson Ross.
- 14 Kennett JP, Elmsstrom K, Penrose N (1985). The last deglaciation in Orca Basin, Gulf of
15 Mexico: high-resolution planktonic foraminiferal changes. Palaeogeography,
16 Palaeoclimatology, Palaeoecology, 50 (2-3): 189-216.
- 17 Laskar J, Wright JD, Boyle EA, Keigwin L (1987). North Atlantic thermohaline
18 circulation during the past 20,000 years linked to high-latitude surface temperature.
19 Nature, 330 (6143): 35.
- 20 Laskar J, Robutel P, Joutel F, Gastineau M, Correia ACM et al. (2004). A long-term
21 numerical solution for the insolation quantities of the Earth. Astronomy and
22 Astrophysics, 428 (1): 261-285.

1 Leckie RM, Wade BS, Pearson PN, Fraass AJ, King DJ et al. (2018). Taxonomy,
2 biostratigraphy, and phylogeny of Oligocene and Early Miocene *Paragloborotalia* and
3 *Parasubbotina*. Cushman Foundation for Foraminiferal Research. In: Wade BS, Olsson
4 RK, Pearson PN, Huber BT, Berggren WA (editors). Atlas of Oligocene Planktonic
5 Foraminifera, Cushman Foundation of Foraminiferal Research, Special Publication, No.
6 46, pp. 29-54.

7 Liu Z, He Y, Jiang Y, Wang H, Liu W et al. (2018). Transient temperature asymmetry
8 between hemispheres in the Palaeogene Atlantic Ocean. *Nature Geoscience*, 11 (9): 656.

9 Maniscalco R, Brunner CA (1998). Neogene and Quaternary planktonic foraminiferal
10 biostratigraphy of the Canary Island Region. In: Weaver PPE, Schmincke HU, Firth JV,
11 Duffield W (editors). Proceedings of the Ocean Drilling Program, Scientific Results, Vol.
12 157, pp. 115-124.

13 Matsui H, Nishi H, Takashima R, Kuroyanagi A, Ikehara M, Takayanagi H, Iryu Y
14 (2016). Changes in the depth habitat of the Oligocene planktic foraminifera
15 (*Dentoglobigerina venezuelana*) induced by thermocline deepening in the eastern
16 equatorial Pacific. *Paleoceanography and Paleoclimatology*, 1, 31(6): 715-31.

17 Mazumder A, Khare N, Govil P (2009). Cosmopolitanism of the planktic foraminiferal
18 species *Globigerinita glutinata*—A testimony by Q-mode cluster analysis. *International*
19 *Journal of Geology*, 1 (3): 1-7.

20 Miller KG, Fairbanks RG (1983). Evidence for Oligocene–Middle Miocene abyssal
21 circulation changes in the western North Atlantic. *Nature* 306, 5940: 250.

22 Miller KG, Aubry MP, Khan MJ, Melillo AJ, Kent DV et al. (1985). Oligocene-Miocene
23 biostratigraphy, magnetostratigraphy, and isotopic stratigraphy of the western North
24 Atlantic. *Geology*, 1, 13 (4): 257-61.

1 Miller KG, Wright JD, Fairbanks RG (1991). Unlocking the ice house: Oligocene-
2 Miocene oxygen isotopes, eustasy, and margin erosion. *Journal of Geophysical Research:*
3 *Solid Earth* 96 (B4): 6829-6848.

4 Moore TC, Wade BS, Westerhold T, Erhardt AM, Coxall HK, et al. (2014). Equatorial
5 Pacific productivity changes near the Eocene-Oligocene boundary. *Paleoceanography*, 29
6 (9): 825-844.

7 Mortyn PG, Charles CD (2003). Planktonic foraminiferal depth habitat and $\delta^{18}O$
8 calibrations: Plankton tow results from the Atlantic sector of the Southern
9 Ocean. *Paleoceanography*, 18 (2).

10 Mountain GS, Tucholke BE (1985). Mesozoic and Cenozoic geology of the US Atlantic
11 continental slope and rise. In: Poag CW (editor), *Geologic Evolution of the United States*
12 *Atlantic Margin*: New York (Van Nostrand Reinhold), pp. 293-341.

13 Nathan SA, Leckie RM (2009). Early history of the Western Pacific Warm Pool during
14 the middle to late Miocene (~13.2–5.8 Ma): Role of sea-level change and implications
15 for equatorial circulation. *Palaeogeography, Palaeoclimatology, Palaeoecology*, 274 (3-
16 4): 140-159.

17 Niebler HS, Hubberten HW, Gersonde R (1999). Oxygen isotope values of planktic
18 foraminifera: a tool for the reconstruction of surface water stratification. In: *Use of*
19 *proxies in paleoceanography*, Springer, Berlin, Heidelberg.

20 Norris RD, Wilson PA, Blum P (2014). The Expedition 342 Scientists: Proceedings
21 IODP, 342. College Station, TX (Integrated Ocean Drilling Program), pp. 165-189, doi.
22 10:2204.

23 Olsson RK, Hemleben C, Huber BT, Berggren WA (2006). Taxonomy, biostratigraphy
24 and phylogeny of Eocene Globigerina, Globoturborotalita, Subbotina and Turborotalita.

1 In: Pearson P, Olsson RK, Huber BT, Hemleben C., Berggren WA (editors.), Atlas of
2 Eocene Planktonic foraminifera, Cushman Foundation Special Publication, No. 41, pp.
3 111-168.

4 Pearson PN, Shackleton NJ (1995). Neogene multispecies planktonic foraminifer stable
5 isotope record, Site 871, Limalok Guyot. In: Haggerty JA, Premoli Silva I, Rack F,
6 McNutt MK (editors), Proceedings of the Ocean Drilling Program, Scientific Results 144,
7 pp. 401-410.

8 Pearson PN, Chaisson WP (1997). Late Paleocene to middle Miocene planktonic
9 foraminifer biostratigraphy of the Ceara Rise. In: Shackleton NJ, Curry WB, Richter C,
10 Bralower TJ (editors), Proceedings of the Ocean Drilling Program Scientific Results,
11 College Station, TX, 154, pp. 33-68.

12 Pearson PN, Shackleton NJ, Weedon GP, Hall MA (1997). Multispecies planktonic
13 foraminifer stable isotope stratigraphy through Oligocene/Miocene boundary climatic
14 cycles, Site 926. Proceedings of the Ocean Drilling Program, Scientific Results 154: 441-
15 450.

16 Pearson PN, Ditchfield PW, Singano J, Harcourt Brown KG, Nicholas CJ et al. (2001).
17 Warm tropical sea surface temperatures in the Late Cretaceous and Eocene epochs.
18 Nature, 413 (6855): 481.

19 Pearson PN, Wade BS (2009). Taxonomy and stable isotope paleoecology of well-
20 preserved planktonic foraminifera from the uppermost Oligocene of Trinidad. The
21 Journal of Foraminiferal Research, 39 (3): 191-217.

22 Pearson PN, Wade BS, Huber BT (2018). Taxonomy, biostratigraphy and phylogeny of
23 Oligocene Globigerinitidae (Dipsidripella, Globigerinita and Tenutella). In: Wade BS,
24 Olsson RK, Pearson PN, Huber BT, Berggren WA, Atlas of Oligocene Planktonic

1 Foraminifera, Cushman Foundation of Foraminiferal Research, Special Publication, v.
2 46, pp. 429-458.

3 Poore RZ, Matthews RK (1984). Oxygen isotope ranking of late Eocene and Oligocene
4 planktonic foraminifers: implications for Oligocene sea-surface temperatures and global
5 ice-volume. *Marine Micropaleontology*, 9 (2): 111-34.

6 Poore RZ (1979). Oligocene through Quaternary planktonic foraminiferal biostratigraphy
7 of the North Atlantic: DSDP Leg 49. *Initial Reports of the Deep Sea Drilling Project*, 49:
8 447-517.

9 Ravelo AC, Fairbanks RG, Philander SG (1990). Reconstructing tropical Atlantic
10 hydrography using planktonic foraminifera and an ocean model. *Paleoceanography*, 5
11 (3): 409-31.

12 Rebesco M, Hernández Molina FJ, Van Rooij D, Wåhlin A (1991). Contourites and
13 associated sediments controlled by deep-water circulation processes: state-of-the-art and
14 future considerations. *Marine Geology*, 352: 111-54.

15 Rohling EJ, De Stigter HC, Vergnaud-Grazzini C, Zaalberg, R (1993). Temporary
16 repopulation by low-oxygen tolerant benthic foraminifera within an upper Pliocene
17 sapropel: evidence for the role of oxygen depletion in the formation of sapropels. *Marine*
18 *Micropaleontology*, 22 (3): 207-219.

19 Rohling EJ, Jorissen FJ, De Stigter HC (1997). 200 year interruption of Holocene
20 sapropel formation in the Adriatic Sea. *Journal of Micropalaeontology*, 16 (2): 97-108.

21 Sautter LR, Thunell RC (1991). Planktonic foraminiferal response to upwelling and
22 seasonal hydrographic conditions; sediment trap results from San Pedro Basin, Southern
23 California Bight. *The Journal of Foraminiferal Research*, 21 (4): 347-63.

1 Schiebel R, Waniek J, Bork M, Hemleben C (2001). Planktic foraminiferal production
2 stimulated by chlorophyll redistribution and entrainment of nutrients. Deep Sea Research
3 Part I: Oceanographic Research Papers, 48 (3): 721-740.

4 Schiebel R, Hemleben C (2017). Planktic foraminifers in the modern ocean (p. 358).
5 Berlin: Springer. Sexton, P.F., Wilson, P.A., Pearson, P.N. (2006). Palaeoecology of late
6 middle Eocene planktic foraminifera and evolutionary implications. Marine
7 Micropaleontology, 60 (1) 1-6.

8 Sexton PF, Wilson PA, Pearson PN (2006). Palaeoecology of late middle Eocene planktic
9 foraminifera and evolutionary implications. Marine Micropaleontology, 60(1): 1-16.

10 Si W, Berggren WA, Aubry MP (2018). Mosaic evolution in the middle Miocene
11 planktonic foraminifera *Fohsella* lineage. Paleobiology, 44 (2): 263-72.

12 Spero HJ, Lea DW (1996). Experimental determination of stable isotope variability in
13 *Globigerina bulloides*: implications for paleoceanographic reconstructions. Marine
14 Micropaleontology, 28 (3-4): 231-46.

15 Spezzaferri S (1994). Planktonic foraminiferal biostratigraphy and taxonomy of the
16 Oligocene and lower Miocene in the oceanic record. An overview. Paleontographia
17 Italica, 81.

18 Spezzaferri S (1995). Planktonic foraminiferal paleoclimatic implications across the
19 Oligocene-Miocene transition in the oceanic record (Atlantic, Indian and South Pacific).
20 Palaeogeography, Palaeoclimatology, Palaeoecology, 114 (1): 43-74.

21 Spezzaferri S (1998). Planktonic foraminifer biostratigraphy and paleoenvironmental
22 implications of Leg 152 Sites (East Greenland Margin). In: Proceedings-Ocean Drilling
23 Program scientific results, National Science Foundation, pp. 161-190.

1 Spezzaferri S, Coric S, Hohenegger J, Rögl F. (2002). Basin-scale paleobiogeography
2 and paleoecology: an example from Karpatian (Latest Burdigalian) benthic and
3 planktonic foraminifera and calcareous nannofossils from the Central Paratethys.
4 *Geobios*, 1 (35): 41-56.

5 Spezzaferri S, Olsson RK, Hemleben C, Wade BS, Coxall HK (2018). Taxonomy,
6 biostratigraphy, and phylogeny of Oligocene and Lower Miocene *Globoturborotalita*. In:
7 Wade BS, Olsson RK, Pearson PN, Huber BT, Berggren WA (editors), Atlas of
8 Oligocene Planktonic Foraminifera. Cushman Foundation for Foraminiferal Research
9 Special Publication, 46, pp. 231-269.

10 Stangeew E (2001). Distribution and Isotopic Composition of Living Planktonic
11 Foraminifera *N. pachyderma* (sinistral) and *T. quinqueloba* in the High Latitude North
12 Atlantic (Doctoral dissertation, Christian-Albrechts Universität Kiel).

13 Stewart DR, Pearson PN, Ditchfield PW, Singano JM (2004). Miocene tropical Indian
14 Ocean temperatures: evidence from three exceptionally preserved foraminiferal
15 assemblages from Tanzania. *Journal of African Earth Sciences*, 40 (3-4): 173-89.

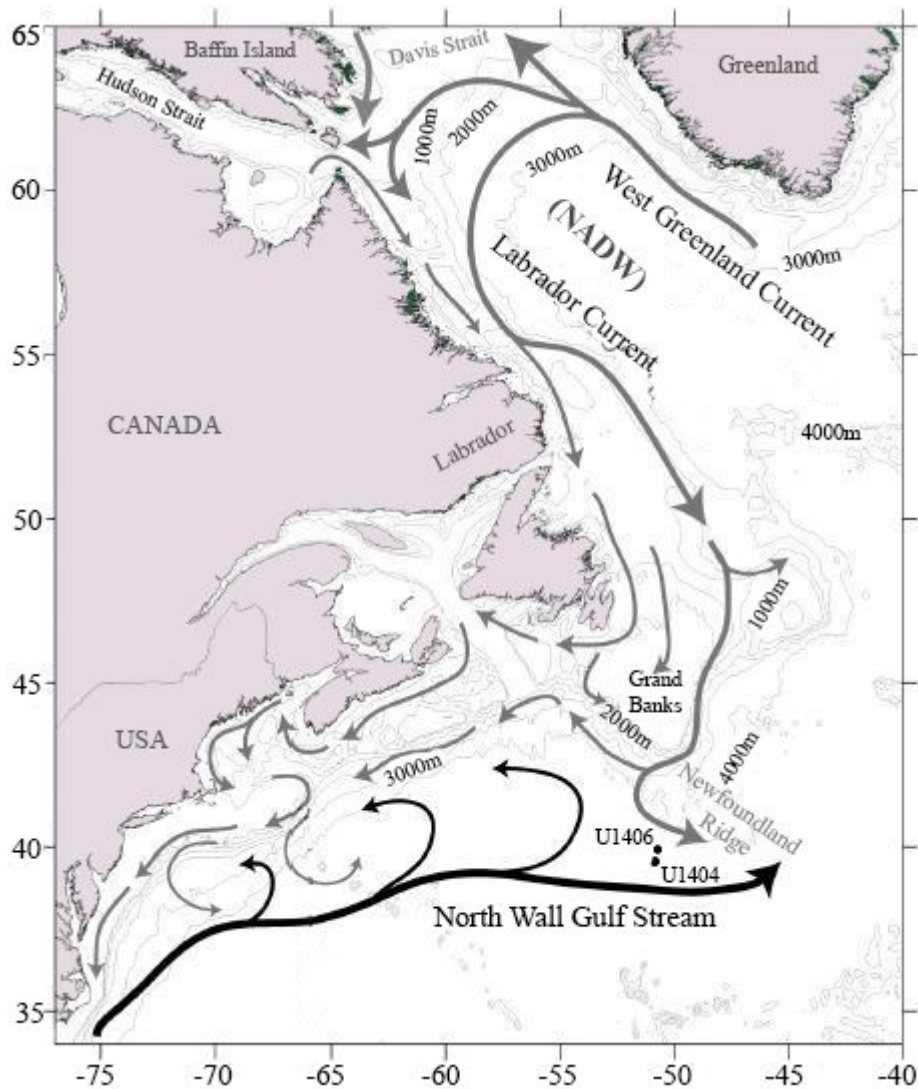
16 Stewart JA, Wilson PA, Edgar KM, Anand P, James RH (2012). Geochemical assessment
17 of the palaeoecology, ontogeny, morphotypic variability and palaeoceanographic utility
18 of “*Dentoglobigerina*” *venezuelana*. *Marine Micropaleontology*, 84-85: 74–86.

19 Stow DA, Faugères JC, Howe JA, Pudsey CJ, Viana AR (2002). Bottom currents,
20 contourites and deep-sea sediment drifts: current state-of-the-art. Geological Society,
21 London, *Memoirs*, 22 (1): 7-20.

22 Townsend DW, Thomas AC, Mayer LM, Thomas MA, Quinlan JA (2004).
23 Oceanography of the northwest Atlantic continental shelf (1, W). In: Robinson, A. R. and

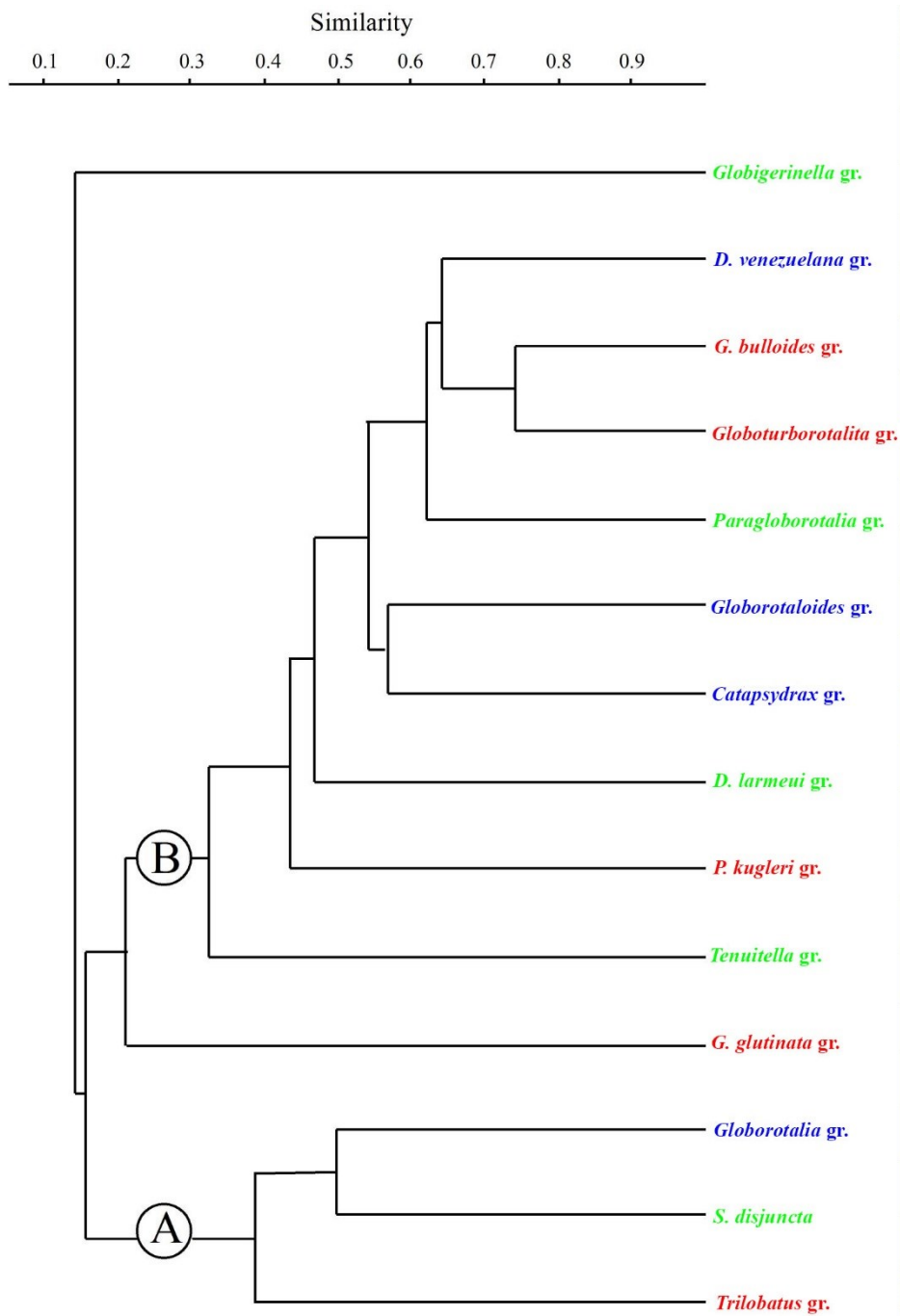
- 1 Brink, H. K. (eds). The sea: the global coastal ocean: interdisciplinary regional studies
2 and syntheses, 14: 119-168.
- 3 Thunell RC, Reynolds L (1984). Sedimentation of planktonic foraminifera: Seasonal
4 changes in species flux in the Panama Basin, *Micropaleontology*, 30: 241–260.
- 5 Tucholke BE, Mountain GS (1979). Seismic stratigraphy, lithostratigraphy and
6 paleosedimentation patterns in the North American Basin. Deep drilling results in the
7 Atlantic Ocean: Continental margins and paleoenvironment, 3: 58-86.
- 8 Van Eijden AJ (1995). Morphology and relative frequency of planktic foraminiferal
9 species in relation to oxygen isotopically inferred depth habitats. *Palaeogeography,*
10 *Palaeoclimatology, Palaeoecology*, 113(2-4): 267-301.
- 11 Van Peer TE, Xuan C, Lippert PC, Liebrand D, Agnini C et al. (2017). Extracting a
12 detailed magnetostratigraphy from weakly magnetized, Oligocene to early Miocene
13 sediment drifts recovered at IODP Site U1406 (Newfoundland margin, northwest Atlantic
14 Ocean). *Geochemistry, Geophysics, Geosystems*, 18 (11): 3910-28.
- 15 Zachos JC, Flower BP, Paul H (1997). Orbitally paced climate oscillations across the
16 Oligocene/Miocene boundary. *Nature*, 388 (6642): 567.
- 17 Zachos JC, Shackleton NJ, Revenaugh JS, Pälike H, Flower BP (2001). Climate response
18 to orbital forcing across the Oligocene-Miocene boundary. *Science*, 292 (5515): 274-8.
- 19 Zachos JC, Dickens GR, Zeebe RE (2008). An early Cenozoic perspective on greenhouse
20 warming and carbon-cycle dynamics. *Nature*, 451 (7176): 279.
- 21 Wade BS, Pälike H (2004). Oligocene climate dynamics. *Paleoceanography*, 19 (4).

- 1 Wade BS, Berggren WA, Olsson RK (2007). The biostratigraphy and paleobiology of
2 Oligocene planktonic foraminifera from the equatorial Pacific Ocean (ODP Site 1218).
3 *Marine Micropaleontology*, 62 (3): 167-79.
- 4 Wade BS, Pearson PN (2008). Planktonic foraminiferal turnover, diversity fluctuations
5 and geochemical signals across the Eocene/Oligocene boundary in Tanzania. *Marine*
6 *Micropaleontology*, 68 (3-4): 244-55.
- 7 Wade BS, Pearson PN, Berggren WA, Pälike H (2011). Review and revision of Cenozoic
8 tropical planktonic foraminiferal biostratigraphy and calibration to the geomagnetic
9 polarity and astronomical time scale. *Earth-Science Reviews*, 104 (1-3): 111-42.
- 10 Wade BS, Houben AJ, Quaijtaal W, Schouten S, Rosenthal Y et al. (2012). Multiproxy
11 record of abrupt sea-surface cooling across the Eocene-Oligocene transition in the Gulf
12 of Mexico. *Geology*, 40 (2): 159-62.
- 13 Wade BS, Pearson PN, Olsson RK, Premoli Silva I, Berggren W et al. (2018). The Atlas
14 of Oligocene Foraminifera, Cushman Foundation, Special Publication 46.
- 15 Wright JD, Miller KG, Fairbanks RG (1991). Evolution of modern deepwater circulation:
16 Evidence from the late Miocene Southern Ocean. *Paleoceanography*, 6 (2): 275-90.



1

2 **Figure 1.** Map of the present oceanic currents insisting in the North Atlantic. The location
 3 of IODP-Site U1406 and IODP-Site U1404 are indicated by the black spots. The main
 4 isobaths are indicated, pinpointing the bathymetry of the studied sequence. All the major
 5 current systems are indicated with the black and grey arrows (figure modified from
 6 Townsend et al., 2004).

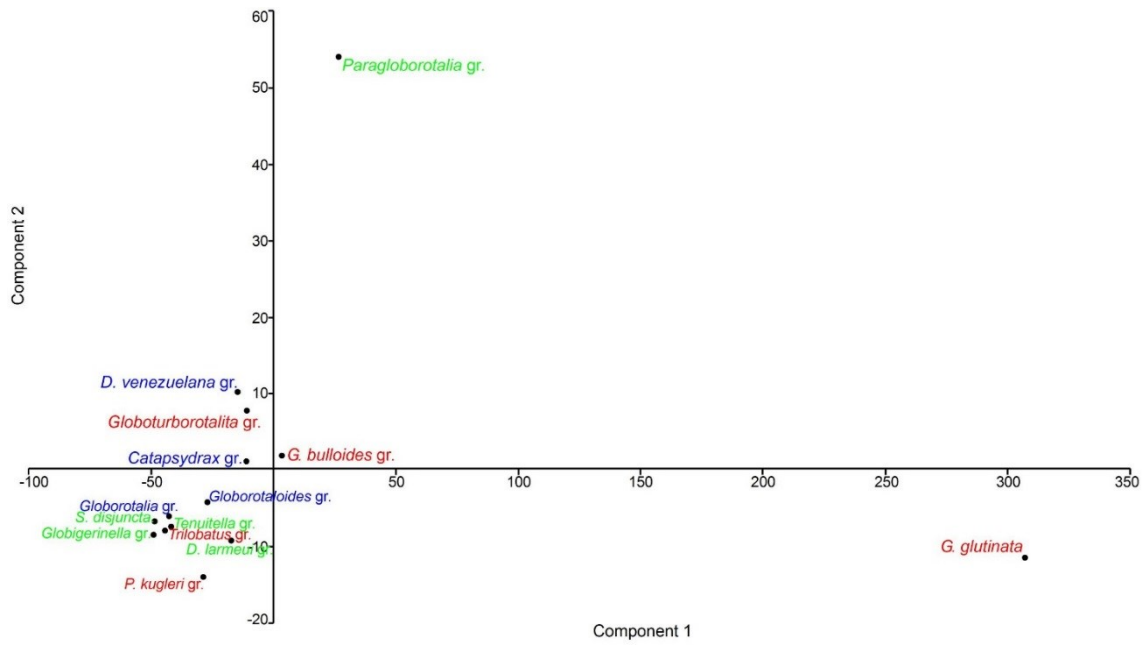


1

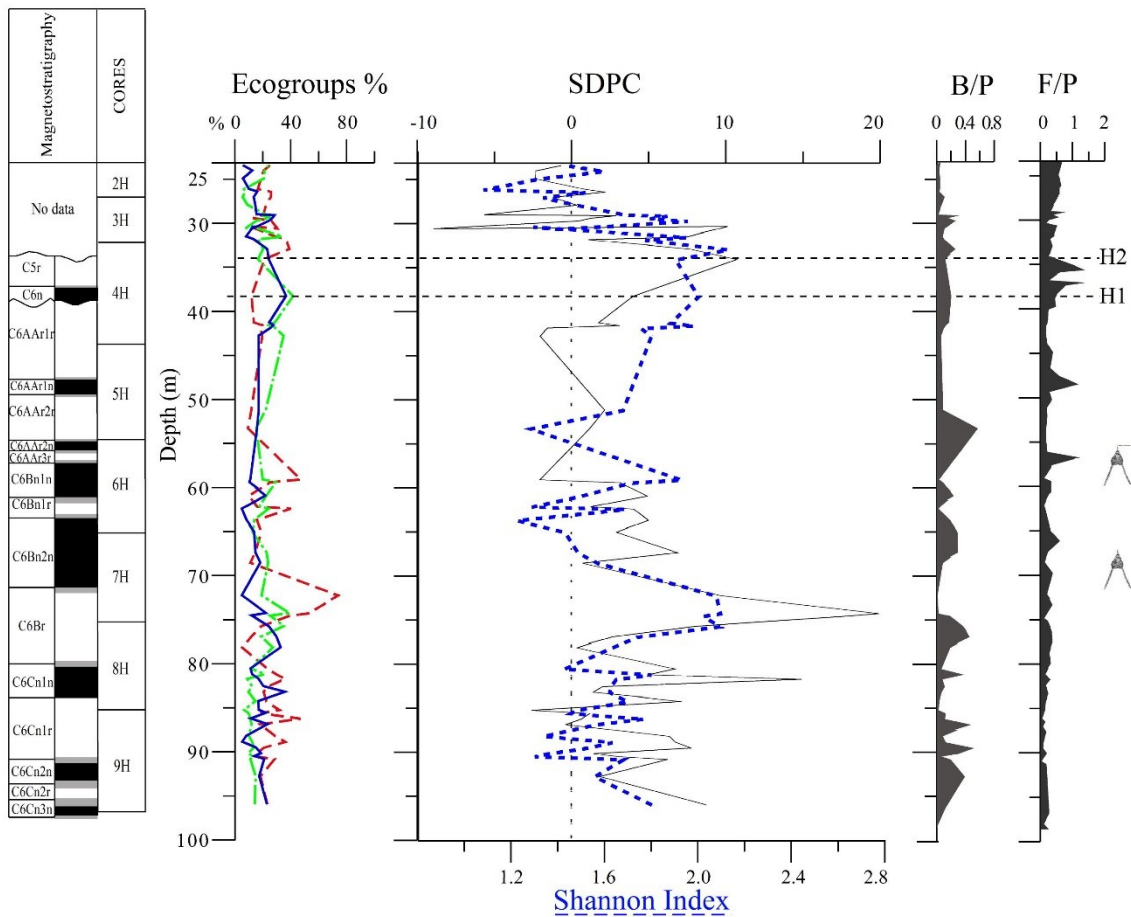
2 **Figure 2.** R-mode cluster dendrogram. The two clusters are indicated by the letters A and

3 B. In red are indicated the species belonging to the Ecogroup 1, in green species from

4 Ecogroup 3 and in blue species from Ecogroup 4.

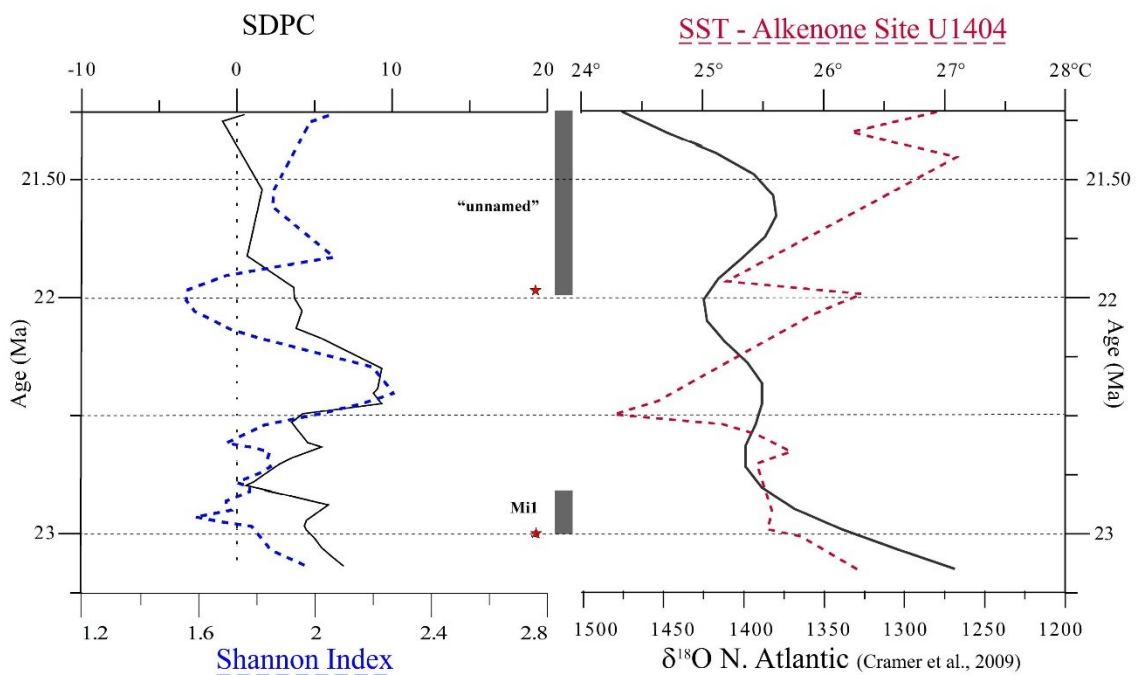


1
 2 **Figure 3** Principal Component Analysis plot. In red are indicated the species belonging
 3 to Ecogroup 1, in green species from Ecogroup 3 and in blue species from Ecogroup 4.



4

1 **Figure 4.** Ecogroup distribution and Shallow Dwellers Paleoclimatic Curve. From left
 2 to right are represented: the magnetostratigraphic model (from Fabbrini et al., 2019), the
 3 three curves (dashed red line: Ecogroup 1; dotted green line: Ecogroup 3; blue line:
 4 Ecogroup 4) describing the ecogroups abundance along the section, the Shallow Dwelling
 5 Paleoclimatic Curve (SDPC - black) and the Shannon Index curve (dashed blue line),
 6 /Benthos/Plankton (B/P) and Fragments/Planktonic (F/P) foraminifera ratios. The
 7 symbols on the righthand side show two intervals characterized by higher presence of
 8 radiolarians. The horizontal dashed lines indicate the two hiatuses (H1 and H2)
 9 recognized by Fabbrini et al. (2019).



10

11 **Figure 5.** Comparison between present data (SDPC and Shannon Index) and SST-
 12 Alkenone (Liu et al., 2018) and $\delta^{18}O$ North Atlantic data (Cramer et al., 2009). On the
 13 left a smoothed SDPC (black line) and the Shannon Index curve (dashed blue) are plotted
 14 versus time (Ma) following the age model proposed by Fabbrini et al. (2019). The graphs
 15 terminate at (age?) owing to hiatus H1. On the right side, data from SST-Alkenone from
 16 IODP-Site U1404 (Liu et al., 2018) – red and dashed line- and the $\delta^{18}O$ North Atlantic
 17 data (Cramer et al., 2009) – in black- are shown. The vertical grey boxes represent the

- 1 regional megahiatuses (Boulila et al., 2011) associated with specific 1.2 Ma obliquity
- 2 nodes (red stars).
- 3 **Table 1.** List of taxa and their ecogroups.

Taxon	Ecogroup	Reference	Climatic index	Reference
<i>Globigerina bulloides</i>	1	Aze et al. (2011)	Cool-temperate	Spezzaferri (1995; 2002; 2018)
<i>Globigerinoides</i> gr.	1	Spezzaferri et al. (2018)	Warm	Hemleben et al. (1989)
<i>Globoturborotalita connecta</i>	1	Spezzaferri et al. (2018)	Warm-temperate	Kennett & Srinivasan (1983)
<i>Globoturborotalita occlusa</i>	1	Stewart et al. (2004)	Warm-temperate	Wade et al. (2018) and references therein
<i>Globoturborotalita ouachitaensis</i>	1	Sexton et al. (2006)	Warm-temperate	Olsson et al. (2006)
<i>Globoturborotalita pseudopraebulloides</i>	1	Pearson and Wade (2009)	Warm-temperate	Wade et al. (2018)
<i>Globoturborotalita woodi</i>	1	Pearson et al. (1997)	Warm-temperate	Spezzaferri (1994; 1995)
<i>Paragloborotalia kugleri</i>	1	Leckie et al. (2018)	Warm-temperate, Upwelling	Leckie et al. (2018)
<i>Paragloborotalia pseudokugleri</i>	1	Leckie et al. (2018) and references therein	Warm-temperate, Upwelling	Spezzaferri (1994)
<i>Trilobatus</i> gr.	1	Spezzaferri et al. (2018)	Warm	Hemleben et al. (1989)
<i>Dentoglobigerina baroemoenensis</i>	3	Wade et al. (2018)	Warm	Kennett & Srinivasan (1983)
<i>Dentoglobigerina globularis</i>	3	Wade et al. (2018)	Warm	Spezzaferri (1994)
<i>Dentoglobigerina larmei</i>	3	Pearson and Wade (2009)	Cosmopolitan	Spezzaferri (1994)
<i>Globigerinella</i> gr.	3	Aze et al. (2011);	Low to mid latitudes	Spezzaferri et al. (2018)
<i>Globoquadrina dehiscens</i>	3	Keller et al. (1985)	Cosmopolitan	Pearson and Shackleton (1995)
<i>Paragloborotalia acrostoma</i>	3	Aze et al. (2011)	Warm-temperate	Leckie et al. (2018)
<i>Paragloborotalia nana</i>	3	Poore and Matthews (1984); Matsui et al. (2016)	Cool-temperate	Spezzaferri (1995)
<i>Paragloborotalia semivera</i>	3	Aze et al. (2011)	Warm-temperate	Kennett & Srinivasan (1983)
<i>Paragloborotalia siakensis</i>	3	Pearson and Wade (2009)	Warm-temperate	Kennett & Srinivasan (1983)
<i>Sphaeroidinellopsis disjuncta</i>	3	Aze et al. (2011)	Low latitudes	Kennett & Srinivasan (1983)
<i>Tenuitella angustiumbilitata</i>	3	Wade et al. (2018)	Warm-temperate	Spezzaferri (1995)
<i>Catapsydrax</i> gr.	4	Aze et al., (2011) and Coxall & Spezzaferri (2018)	Global, upwelling	Coxall & Spezzaferri (2018)
<i>Dentoglobigerina binaiensis</i>	4	Pearson and Shackleton (1995)	Warm	Pearson and Chaisson (1997)
<i>Dentoglobigerina tripartita</i>	4	Van Eijden & Ganssen (1995)	Cosmopolitan	Wade et al. (2018)
<i>Dentoglobigerina venezuelana</i>	4	Wade et al., (2018)	Warm-temperate	Kennett & Srinivasan (1983)
<i>Globorotalia</i> gr.	4	Aze et al. (2011)	Warm-temperate	Kennett & Srinivasan (1983)
<i>Globorotaloides</i> gr.	4	Poore and Matthews (1984)	Cool, Upwelling	Spezzaferri (1995)
<i>Globigerinita glutinata</i>	-	Pearson (2001,2009)	Cool-temperate/global	Spezzaferri (1995)